Development of a Small Legged Wall Climbing Robot with Passive Suction Cups

Soichiro KAWASAKI*[1] and Koki KIKUCHI*[1]
*1 The Department of Advanced Robotics, Chiba Institute of Technology
2-17-1 Tsudanuma, Narashino, Chiba 275-0016, JAPAN
S1376008MV@it-chiba.ac.jp, kikut@ieee.org

Abstract
In this paper, we develop a small hexapod robot with passive suction cups and realize vertical wall climbing. The passive adhesion mechanisms make the robotic system small and simple, since it requires neither energy nor an additional actuator to stay on the vertical wall. Above all, the passive suction cup is suited to vertical wall climbing because it is strongly attached to a wall with a smooth surface and is simply detached from it by pulling the edge of the cup. These characteristics are intensified according to the decreasing robotic scale. In this study, we developed a small wall climbing robot 12 cm long and 34 g in weight and driven by single degree-of-freedom linkage legs based on the scale effect. Here, the linkage mechanism optimized by a genetic algorithm provided the effective trajectory of the legs and the attachment-detachment cycle. As a result, the robot traveled on the ground at a velocity of 2.7 cm/s and climbed on the vertical wall at a velocity of 2.2 cm/s.
Keywords: legged robot, vertical wall climbing, suction cup, scale effect

1 Introduction
A wall climbing robot is promising for various applications such as inspecting a tall building and cleaning a window, for example. To stay on the vertical wall, there are mainly two mechanisms: active and passive adhesions. While the active adhesion mechanism [1]-[4] uses negative pressure or electrostatic force to exert strong adhesion force and to control the attachment and detachment quickly, it requires some kind of additional actuator, such as a vacuum pump, and always consumes energy to just stay on the wall. On the other hand, the passive adhesion mechanism [5]-[9], such as the adhesive substance used by an ant or the passive suction cups used by an octopus, can generate large adhesion force without a power supply and does not need an additional actuator to change the attachment and detachment phases. This property makes the robotic system small and simple. Since the weight is proportional to the mass, i.e., the length cubed, the smaller the body size, the more advantageous it is for vertical wall climbing. From this viewpoint, the passive adhesive mechanism is suited to a small wall climbing robot moving with a few degrees of freedom (DOF). In particular, a passive suction cup has unique characteristics such as the edge of the suction cup is detached easily and the suction cup exerts far larger adhesion force than pushing force to attach it. Moreover, it can simplify control of the attachment and the detachment mechanism. There are several types of vertical wall climbing mechanisms using such a suction cup [9], [10]. The crawler type is simple, but it requires an additional mechanism to push the suction cup. Although the legged type does not require the additional pushing mechanism, it is difficult to generate an effective leg trajectory and to design a simple and light attachment-detachment mechanism.

From this point of view, we develop a small legged wall climbing robot using passive suction cups in this study. Here, to use the scale effect advantage, we fabricate the hexapod robot based on the *cm*-scale. Then we optimize the leg trajectory by a genetic algorithm (GA) and design the simple and light detachment mechanism by which a string pulls the edge of the suction cup and peels it from the wall surface. Finally, we realize ground travel and vertical wall climbing by passive adhesion.

2 Robotic system
2.1 Robot overview
Figure 1 shows a model of the wall climbing robot. The robot has six legs assembled by a four-bar linkage mechanism. The link parameter, i.e., the combination of the link length and the position, generates the leg tip trajectory and the posture. Here, L means the body length. The diameter of the suction cup is set to $L/6$ to avoid collision between the fore and hind suction cups. The body width, $L/3$, and the body height, $L/5$, are

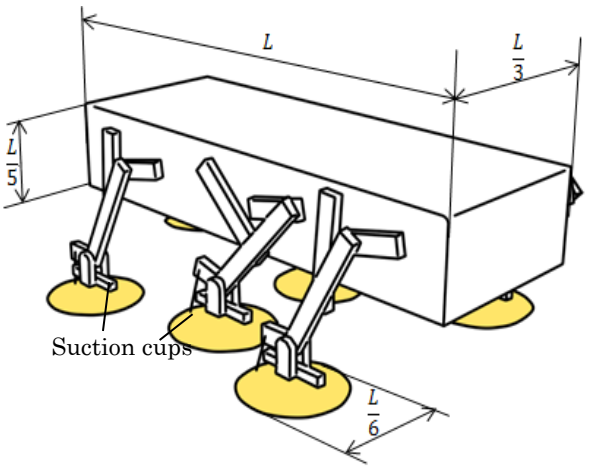

Fig. 1 Robot model

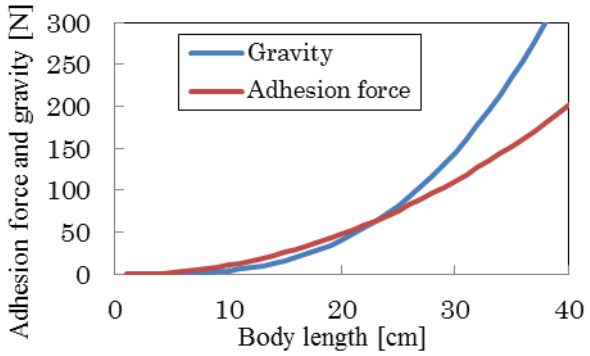

Fig. 2 Adhesion force and gravity against body length

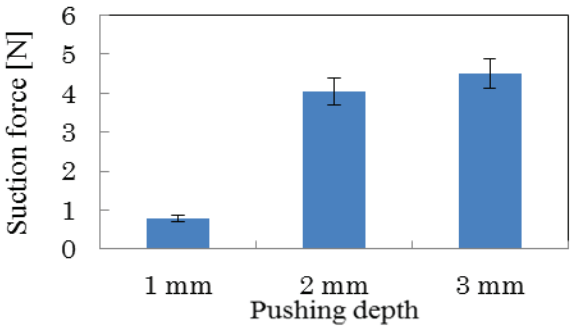

Fig. 3 Relationship between suction force and pushing depth

defined based on the space for the battery and actuators. An alternating tripod gait is adopted for locomotion and is driven by a single DOF. Since this gait always supports the body by three or more legs, it stabilizes the body posture.

2.2 Adhesion mechanism by the suction cup

The robot adheres to the wall by the negative pressure of the suction cup. The maximum adhesion force, F_{max}, by three suction cups is provided by

$$F_{max} = 3\pi\mu\left(\frac{d}{2}\right)^2 P_0 \Delta V \qquad (1)$$

where μ is the friction coefficient, d is the diameter (L/6), P_0 is the atmospheric pressure per unit area (10.03 N/cm^2), and ΔV is the ratio between the inner volumes of the initial and deformed suction cups (generally 0.05). **Figure 2** shows the relationship of adhesion force and gravity with the length. Here, the body weight is calculated by $\rho L(L/3)(L/5)$ and the material is styrene acrylonitrile butadiene copolymers (ρ=1.05). The friction coefficient is set to 0.67 based on our pilot experiment. From this figure, we can see that a robot less than almost 22 cm can sufficiently generate the adhesion force to stay on the vertical wall. In this study, we chose L to be almost 10 cm (the diameter of the suction cup L/6=1.7) based on a margin of safety ratio of 2.

Next, we investigate the relationship between the generative suction force and the pushing depth from the initial shape of the suction cup. Note that we define the force to detach from the surface as the suction force and the force to move away from the surface as the adhesion force. In the case of vertical wall climbing, the suction force is perpendicular to the wall surface and the adhesion force is parallel to it. Hence, let the former be f, the latter be μf. **Figure 3** shows the experimental result of the relationship between the generative suction force and the pushing depth. Here, the height of the inner space of the suction cup is 5 mm. This figure shows that a pushing depth greater than 2 mm can generate enough suction force. Therefore, the leg must push the suction cup at least 2 mm from the contact point of the bottom face at the beginning of the supporting leg phase. **Figure 4** shows the relationship

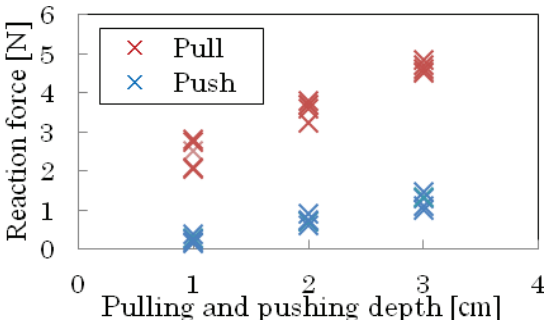

Fig. 4 Property of suction cup

between the reaction force and pushing or pulling depth perpendicular to the wall surface. To avoid falling, the resultant force, calculated by multiplying the friction coefficient by the force and subtracting the pushing force from the pulling force, must be greater than the gravity, when the supporting and swinging legs are interchanged. From the figure, we can see that the pushing depth of 2 mm generates enough suction force even during such a switching phase. From the above discussion, we set the pushing depth to be 2 mm.

2.3 Attachment and detachment mechanisms

To develop a small and simple wall climbing system, we design the periodical attachment and detachment mechanism by which the leg pushes the suction cup to the wall at the beginning of the supporting leg phase and the string pulls the edge of the suction cup at the beginning of the swinging leg phase. **Figure 5**(a) shows our proposed detachment mechanism with the suction supporter. The nylon string connected from the leg tip peels the edge of the suction cup and detaches the whole suction cup from the wall surface. We can control the detachment phase by adjusting the ankle angle against the wall, as mentioned below. Note that, in the case that the supporter does not ground the wall and inclines, the robot cannot concentrate the peeling stress on the edge of the suction cup, and then control of the detachment phase becomes difficult (**Fig. 5**(b)). **Figure 6** shows the attachment and detachment sequence. Every single leg during the alternating tripod gait behaves as follows:

(1) The swinging leg touches the wall. Here, it does not yet exert the adhesion force.
(2) The swinging leg pushes the suction cup toward the wall.

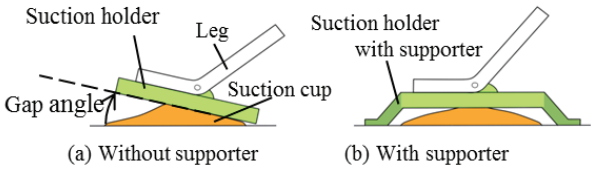

Fig. 5 Attachment and detachment mechanism

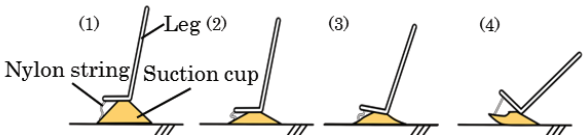

Fig. 6 Attachment and detachment sequence

(3) The leg is supported by the adhesion force of the suction cup.
(4) The suction cup is peeled from the wall by pulling the string connected to the edge. Then the leg becomes the swinging leg.

Following the definition of Nagakubo *et al*. [11], we define each section (1) - (2), (2) - (3), (3) - (4), and (4) - (1) as the pre-attach phase, leg-in-support phase, pre-detach phase, and leg-in-return phase, respectively. This attachment and detachment interval is designed by the linkage parameter. The stride of the leg, the reaction force, and the velocity are determined by this sequence.

2.4 Four-bar linkage mechanism

The legs are driven by a single-DOF four-bar linkage mechanism, as shown in **Fig. 7**. Joints O and A are fixed on the coordinates (0,0) and (a_x, a_y), respectively. Link L_1 rotates and the angle is θ_0. Ankle position P and angles θ_1 and θ_2 are geometrically determined by the variable θ_0 and the link lengths L_1, L_2, L_3, and L_4. Angle α is the ankle angle designed in advance, and ϕ is the ankle angle for the wall and becomes the peeling angle when the leg touches the ground. The leg trajectory, the leg posture (the ankle angle for the wall), and the attachment-detachment interval designed by the linkage parameter are very important for legged locomotion. Additionally, the reaction force determined by this parameter is also important. Here, we formulate the trajectory of the leg and the torque of the crank link. The ankle position is provided by

$$\begin{aligned} x &= L_1\cos\theta_0 + (L_2+L_3)\cos(\theta_0+\theta_1) \\ y &= L_1\sin\theta_0 + (L_2+L_3)\sin(\theta_0+\theta_1) \end{aligned} . \quad (2)$$

From the geometric relationship, we obtain the position C described by

$$\begin{aligned} &L_1\cos\theta_0 + L_2\cos(\theta_0+\theta_1) = a_x + L_4\cos(\theta_2+\beta+\pi) \\ &L_1\sin\theta_0 + L_2\sin(\theta_0+\theta_1) = a_y + L_4\sin(\theta_2+\beta+\pi) \\ &\quad where \quad \tan(\beta) = a_y / a_x \end{aligned} . \quad (3)$$

Here, we define the five important indices for legged

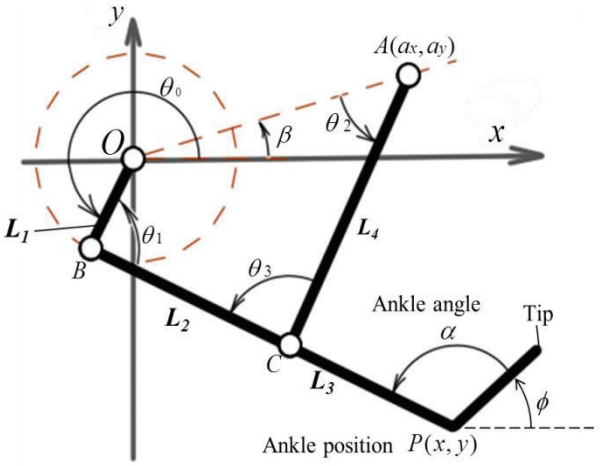

Fig. 7 Parameters for four-bar linkage mechanism

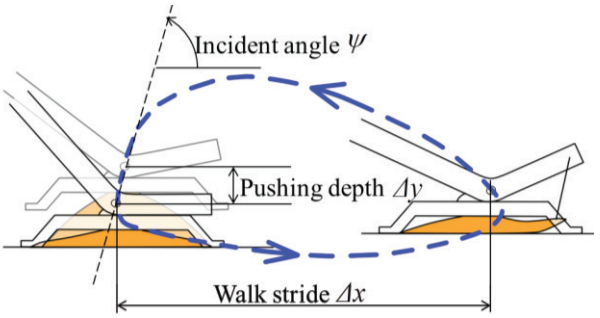

Fig. 8 Ankle trajectory, stride, and incident angle

locomotion by a suction cup. The pre-attach interval $\Delta\phi$ is the difference of the ankle angle for the wall from the leg touch to the leg detachment. When this angle is small, the leg cannot push the suction cup sufficiently. The incident angle ψ is the angle between the ground and the pushing direction of the suction cup, as shown in **Fig. 8**. The more perpendicular the value of ψ is to the wall, the better. Note that the interval was set to 5 deg in this study to ensure the pushing depth of 2 mm. The walk stride Δx is the displacement from the touching point to the detaching point and the pushing depth Δy determines the suction force, as mentioned in section 2.2. Next, the torque around the crank shaft, T_0, is provided as the outer product of the position vector OP and the reaction force vector, as shown in **Fig. 4**,

$$T_0 = [L_1\cos\theta_0 + (L_2+L_3)\cos(\theta_0+\theta_1)]F . \quad (4)$$

A thin shaft for the small linkage mechanism cannot transmit a large torque due to the slippage, etc. Thus, we set the maximum torque of the crank shaft to less than some threshold value.

Table 1 Linkage parameters

L_1 [mm]	L_2 [mm]	L_3 [mm]	L_4 [mm]	L_5 [mm]	α [deg]	a_x [mm]	a_x [mm]
9.0	13.3	3.0	13.4	5.0	116	13	10

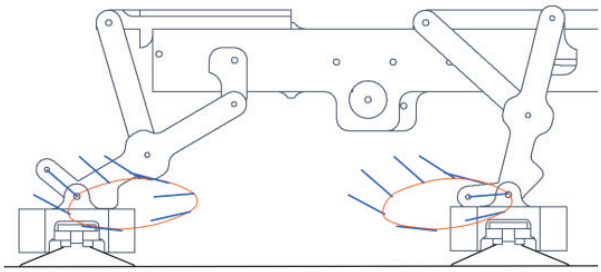

Fig. 9 Leg trajectory and posture

3 Linkage parameter optimization

To search for the linkage parameter that optimizes the above conditions, we used a stochastic searching method as the genetic algorithm (GA). The fitness function is

$$E = k_1 \frac{\Delta x \Delta y}{1 + \left| \frac{1}{2}\pi - \psi \right|} - k_2 T_o + k_3 \Delta \phi \qquad (5)$$

where k_1, k_2, and k_3 are constants ($k_1 + k_2 + k_3 = 1$). In this study, based on the pilot experiments, we set these constants as 1/16, 5/16, and 10/16, respectively. The first term on the right side of (5) expresses the ratio between the area of supporting leg motion and the incident angle. Thus, the larger the area is, the better. The more the incident angle is perpendicular, the better. From the second term, the smaller the torque of the crank shaft is, the better. From the third term, the longer the pre-attach interval is, the better. The linkage parameters described as a chromosome in the GA are the four link lengths L_1, L_2, L_3, and L_4, the ankle angle, and the A position, (a_x, a_y). The GA parameters are population 200, generation 100, crossover ratio 0.3, mutation ratio 0.3, and selection ratio 0.7. Note that we set the maximum value of T_0 as 0.001 Nm and eliminate the chromosome that is more than that value as the fatal one. **Table 1** shows the obtained linkage parameters and **Fig. 9** illustrates the leg trajectory and posture. In this paper, we used these results and fabricated the robot.

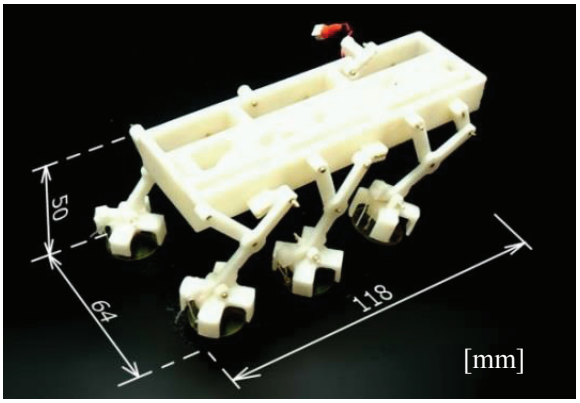

Fig. 10 Small legged wall climbing robot

4 Wall climbing experiment

4.1 Prototype of wall climbing robot

We fabricated a prototype of the wall climbing robot based on the obtained linkage parameters (**Fig. 10**). The robot is 118 mm in length, 64 mm in width, 50 mm in height, and 34 g in weight. The alternating tripod gait is achieved by a single coreless motor of 0.46 W. The reduction gear ratio is 168.8:1. In this study, we used an external power supply.

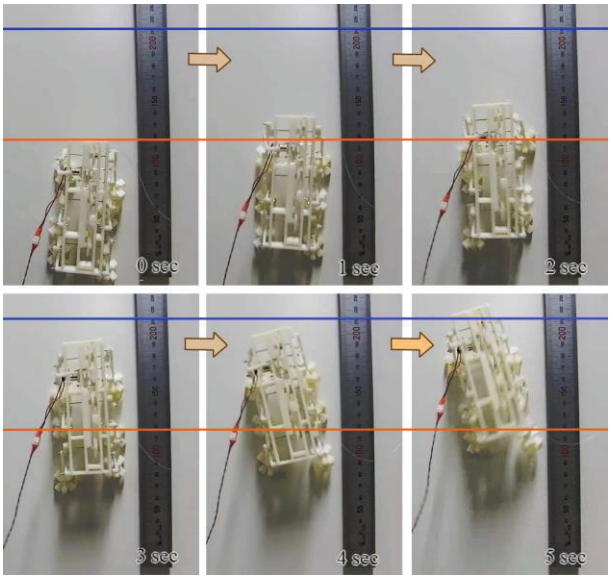

Fig. 11 An example of vertical wall climbing

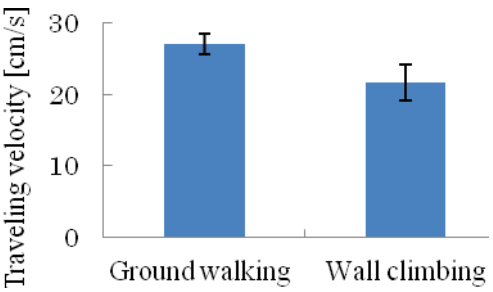

Fig. 12 Traveling velocities

4.2 Prototype of wall climbing robot

We performed the experiments on the ground and on a vertical wall with a smooth surface. **Figure 11** shows an example of the vertical wall climbing experiment and **Fig. 12** shows the velocities for the ground and the vertical wall. As the results of 10 experiments, the robot traveled horizontally at a velocity of 2.7 cm/s (std. dev. 1.4) and climbed vertically at a velocity of 2.1 cm/s (std. dev. 2.5), respectively. The proposed robot did not fall from the wall and climbed stably. However, the robot shifted 2.3 cm to the left during 10.0 cm of travel.

7 Conclusions

In this study, we developed a small legged wall climbing robot using passive suction cups. The

proposed attachment and detachment mechanism makes not only the robot small but also simplifies the control. The leg trajectory by the four-bar linkage mechanism is designed by a genetic algorithm and generates stable locomotion. The result showed that the robot traveled on the ground at a velocity of 2.7 cm/s and climbed on the vertical wall at a velocity of 2.1 cm/s.

In future work, we intend to improve the locomotion velocity and the design of the steering mechanism.

References

[1]Kim, H., Kim, D., Yang, H., Lee, K., Seo, K., Chang, D., and Kim, J., "Development of a Wall-climbing Robot Using a Tracked Wheel Mechanism." Journal of mechanical science and technology, Vol.22, No.8, (2008), pp.1490-1498.

[2] Tohru Miyake Hidenori Ishihara, and Tatsuya Tomino, "Vacuum-based Wet Adhesion System for Wall Climbing Robots - Lubricating Action and Seal Action by the Liquid -", IEEE International Conference on Robotics and Biomimetics, (2009), pp.21-26.

[3] Wagner, M., Chen, X., Nayyerloo, M., Wang, W., and Chase, J. G., "A Novel Wall Climbing Robot Based on Bernoulli Effect", IEEE/ASME International Conference on Mechatronics and Embedded Systems and Applications, (2008), pp. 210-215.

[4] Wang, H., Yamamoto, A., and Higuchi, T., "Electrostatic-motor-driven Electroadhesive Robot", IEEE/RSJ International Conference on Intelligent Robots and Systems, (2012), pp. 914-919.

[5] Federle, W., Werner, B., and Bert, H., "Biomechanics of ant adhesive pads: frictional forces are rate - and temperature - dependent", The Journal of Experimental Biology 206, (2004), pp.67-74.

[6] Unver, O., and Sitti, M., "Tankbot: A Miniature, Peeling Based Climber on Rough and Smooth Surfaces", IEEE International Conference on Robotics and Automation, (2009), pp. 2282-2287.

[7] Wang, K., Wang, W., and Zhang, H., "The Mechanical Properties of a Wall-Climbing Caterpillar Robot: Analysis and Experiment", International Journal of Advanced Robotic System, INTECH, (2013).

[8]Sangbae, K., Spenko, M., Trujillo, S., Heyneman, B., Santos, D., Cutkosky, M.R., "Smooth Vertical Surface Climbing With Directional Adhesion", IEEE TRANSACTIONS ON ROBOTICS, Vol.24, No.1, (2008), pp.65-74.

[9] Murphy, M.P., Tso, W., Tanzini, M., Sitti, M., "Waalbot: An Agile Small-Scale Wall Climbing Robot Utilizing Pressure Sensitive Adhesives", IEEE/RSJ International Conference on Intelligent Robotics and Systems, IEEE, (2006), pp.3411-3416.

[10] Yu, Y., and Shugen, M., "A Wall-Climbing Robot without any Active Suction Mechanisms", IEEE International Conference on Robotics and Biomimetics, (2011), pp.2014-2019.

[11] Akihiko, N., Shigeo, H., "Wall Gait: A Standard Gait for the Quadruped Wall-Climbing Robot", The Japan Society of Mechanical Engineers, C, Vol.61, No.588, (1995), pp.3326-3334.

Received on December 31, 2013.
Accepted on February 28, 2014